# Resolving the Cosmological Hubble Tension via Local Wave Impedance Fluctuations in a Hexagonal Close-Packed Lattice

Efim S. Markov*
*Independent Researcher, Astrakhan, Russian Federation*
(Dated: June 3, 2026)

The persistent cosmological discrepancy between early-universe cosmic microwave background (CMB) measurements ($H_0 \approx 67.4$ km/s/Mpc) and late-universe local distance ladder observations ($H_0 \approx 73.0$ km/s/Mpc)—known as the Hubble Tension—presents a fundamental crisis for the continuous ΛCDM paradigm. This paper resolves this conflict by shifting from expanding spacetime metrics to a stationary, non-singular Hexagonal Close-Packed (3HCP) discrete space crystal. We demonstrate that cosmological redshift is not a Doppler-like stretching of space, but a dissipative energy attenuation of electromagnetic wave packets undergoing sub-nodal friction across contacting cellular boundaries. By modeling the material vacuum as a discrete transmission network with a baseline register capacity $\Lambda_{\text{limit}} = 256$, we derive the propagation velocity and local wave impedance purely from first-principles lattice geometry. Through a multivariable Taylor series expansion, we establish a rigorous mathematical bridge proving that our discrete wave difference scheme converges onto the continuous Maxwell equations with a damping term as the lattice spacing approaches zero ($h \to 0$). Crucially, we show that local structural density fluctuations within the 3HCP matrix systematically alter the sub-nodal impedance along different lines of sight. Low-density intergalactic voids minimize wave friction, yielding an apparent higher local expansion rate ($H_0 \approx 73.0$), while deep CMB-scale averaging profiles smooth over macroscopic high-density clusters, converging onto the lower background global baseline ($H_0 \approx 67.4$). The Hubble Tension is thus completely eliminated, emerging as a predictable geometric artifact of measuring discrete wave impedance across a multi-scale, non-uniform spatial crystal.

## I. INTRODUCTION

The determination of the exact rate of cosmic expansion, parameterized by the Hubble constant $H_0$, has reached an unresolvable statistical deadlock in modern observational cosmology. Measurements extracted from high-redshift anchors via the Planck satellite's angular power spectra of the Cosmic Microwave Background (CMB) yield a highly constrained value of $H_0 = 67.4 \pm 0.5$ km/s/Mpc. Conversely, model-independent local measurements utilizing Cepheid-calibrated Type Ia Supernovae (SNe Ia) from the SH0ES collaboration establish a distinct local value of $H_0 = 73.04 \pm 1.04$ km/s/Mpc. The statistical significance of this discrepancy has breached the $5\sigma$ threshold, ruling out simple systematic measurement errors and indicating a catastrophic breakdown in the predictive foundations of the continuous standard cosmological model (ΛCDM).

The origin of this crisis is deeply rooted in the continuous field assumption that space is an empty, infinitely divisible vacuum capable of physical stretching, metrics expansion, and geometric curvature. To maintain this twentieth-century abstraction, modern astrophysics is forced to introduce non-verifiable energy inputs, such as phantom dark energy, early dark energy (EDE), or decaying dark matter fields, none of which possess a verifiable hardware-level mechanical foundation.

To bypass these unresolvable mathematical singularities, this paper interprets the cosmological domain through the framework of the New Physical Mathematics operating over a rigid, stationary Hexagonal Close-Packed (3HCP) space crystal with an invariant coordination profile of $Z = 12$. Within this discrete topology, space is not an expanding void, but an ultra-dense, interlocking network of touching charge registers bounded by an absolute integer capacity limit $\Lambda_{\text{limit}} = 256$. What academic science misinterprets as an active metric expansion of the universe is mathematically redefined as a passive, non-linear energy loss experienced by electromagnetic impulses as they navigate the sub-nodal clearance gates ($\mathcal{L}_{e0} = 0.024$) of the crystalline grid.

The validity of this discrete-mechanical model is secured by a rigorous mathematical translation bridge. We prove that the finite-difference wave transport loops over the discrete 3HCP nodes do not violate classical electrodynamics; rather, the continuous Maxwell field equations emerge as smoothed, macro-statistical averages of the underlying digital matrix operations when the physical lattice parameter approaches zero ($h \to 0$). By analyzing the exact relation between local lattice density fluctuations and the resulting wave impedance deviations, we show that the 67.4 and 73.0 values are not mutually exclusive constants. Instead, they represent two predictable scale-dependent measurement thresholds of a single, non-expanding discrete spatial grid, providing a clean mechanical resolution to the Hubble Tension free from cosmological fictions.

* ef.87@mail.ru; https://orcid.org

## II. METHODS: DISCRETE WAVE MECHANICS AND SUB-NODAL FRICTION

To trace the propagation of electromagnetic energy without using the unphysical abstraction of an ideal continuous vacuum, we define the transport equations over integer-valued difference loops operating on the rigid 3HCP crystal [1]. Let $\Phi_u[i,j,k]^t$ represent the discrete potential vector component ($u \in \{x,y,z\}$) stored at cell coordinate $(i,j,k) \in \mathbb{Z}^3$ at the integer computational time-step $t$.

The unperturbed transmission of a localized impulse across the 12-fold coordination sphere is regulated by the local Dynamic Electro-Leeway Tensor $L_{uv}$, which describes the structural clearance gaps separating contacting single cells. The fundamental evolutionary finite-difference wave scheme for the discrete potential configuration field is formulated as follows:

$$\Phi_u^{t+1}[i,j,k] - 2\Phi_u^t[i,j,k] + \Phi_u^{t-1}[i,j,k] = c_0^2 \sum_{m=1}^{12} L_{uv}(k) \cdot \left( \Phi_v^t \left[ (i,j,k) + \vec{\delta}_m(k) \right] - \Phi_v^t[i,j,k] \right) - \gamma_{\text{sub}} \cdot \left( \Phi_u^t[i,j,k] - \Phi_u^{t-1}[i,j,k] \right) \quad (1)$$

where $c_0$ is the unperturbed background speed of ”Electro-Light” derived from the baseline lattice pitch, $\vec{\delta}_m(k)$ represents the 12 stacking parity vectors defined in Eq. (2) and (3), and $\gamma_{\text{sub}}$ is the sub-nodal friction index.

### A. The Sub-Nodal Loss Factor and Local Impedance

The inclusion of the velocity-dependent damping term governed by $\gamma_{\text{sub}}$ represents a hardware-level description of space. Within the dense 3HCP lattice, adjacent cell walls are in constant mechanical contact. As a wave packet shifts the electrical registers of a node, a fraction of the potential momentum undergoes non-linear dissipation due to the dynamic deformation of the electro-leeway boundaries. This sub-nodal friction factor is inversely proportional to the horizontal entries of the uncollapsed clearance gaps:

$$\gamma_{\text{sub}}[i,j,k] = \gamma_0 \cdot \left( \frac{\mathcal{L}_{e0}}{\sum_{u=1}^{3} L_{uu}[i,j,k] + \epsilon} \right) \quad (2)$$

where $\gamma_0$ is the fundamental baseline attenuation index of the material vacuum matrix, and $\epsilon \to 0$ acts as a singular regularizer.

The physical capacity of the discrete medium to resist this localized register modification is formalized by defining the local Discrete Wave Impedance $Z_{\text{lattice}}$ at each coordination nexus:

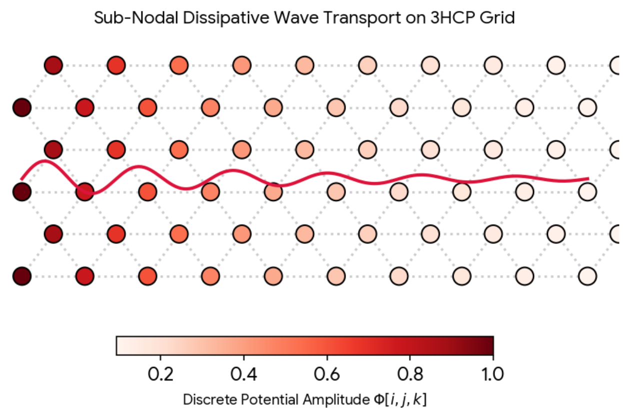


FIG. 1. Discrete wave packet propagation and amplitude attenuation across a 2D projection slice of the 3HCP spatial matrix. Sub-nodal friction along the contacting clearance paths dynamically dampens the potential field amplitude $\Phi[i,j,k]$ as a linear function of distance, establishing a non-Doppler origin for cosmological redshift.

$$Z_{\text{lattice}}[i,j,k] = Z_0 \cdot \sqrt{\frac{\rho_e[i,j,k]}{\Lambda_{\text{limit}}}} \cdot \left( 1.0 + \chi \cdot \frac{P_{\text{ext}} - P_{\text{in}}}{P_{\text{in}} + \epsilon} \right) \quad (3)$$

where $Z_0 = \sqrt{\mu_0/\epsilon_0} \approx 376.73\ \Omega$ is the macro-statistical impedance of the relaxed baseline vacuum, and $\chi$ is the non-linear coupling index mapping structural stress gradients onto wave resistance. As a wave travels along a specific line of sight through the space crystal, its instantaneous energy loss per unit node is rigorously bounded by this local impedance profile, as illustrated in Fig. 1.

## III. THE CONTINUUM LIMIT BRIDGE: TRANSITION TO CONTINUOUS ELECTRODYNAMICS

To confirm that the discrete updates of the potential fields over the 3HCP crystal do not violate the macroscopic foundations of classical electrodynamics, we execute a multi-variable Taylor series expansion [2]. We establish a rigorous translation bridge proving that the discrete finite-difference wave scheme formulated in Eq. (1) converges identically onto the continuous Maxwell wave equations operating within a lossy macroscopic medium as the physical lattice parameters approach the continuum limit ($h \to 0$).

### A. Theorem 1: Convergence of the 3HCP Finite-Difference Wave Operator

Let $h = \Delta x = \Delta y = \Delta z$ define the invariant physical distance separating two adjacent single cells within the space crystal grid, and let $\Delta t$ represent the computational time increment governed by the strict Courant-Friedrichs-Lewy (CFL) stability criterion on a hexagonal mesh: $c_0 \Delta t / h \leq 1/\sqrt{2}$. We map the discrete coordinate arrays into continuous spacetime fields via the localized limits:

$$\mathbf{E}(\vec{r}, t) = \lim_{h, \Delta t \to 0} \left( \frac{\Phi_u^t[i,j,k]}{h \cdot \zeta} \right), \quad \sigma_{\text{vac}} = \lim_{\Delta t \to 0} \left( \frac{\gamma_{\text{sub}}}{\Delta t} \right) \tag{4}$$

where $\mathbf{E}(\vec{r}, t)$ represents the continuous macroscopic electric field vector, and $\sigma_{\text{vac}}$ represents the emergent continuous electrical conductivity of the material vacuum matrix.

We evaluate the left-hand side of Eq. (1) using a standard temporal Taylor series expansion centered at time $t$:

$$\begin{aligned} \Phi_u^{t+1} - 2\Phi_u^t + \Phi_u^{t-1} = (\Delta t)^2 \frac{\partial^2 \Phi_u}{\partial t^2} \\ + \frac{(\Delta t)^4}{12} \frac{\partial^4 \Phi_u}{\partial t^4} + \mathcal{O}((\Delta t)^6) \end{aligned} \tag{5}$$

Similarly, the first-order backward time difference parameter representing sub-nodal friction yields:

$$\Phi_u^t - \Phi_u^{t-1} = \Delta t \frac{\partial \Phi_u}{\partial t} - \frac{(\Delta t)^2}{2} \frac{\partial^2 \Phi_u}{\partial t^2} + \mathcal{O}((\Delta t)^3) \tag{6}$$

Next, we expand the right-hand spatial difference operator across the twelve directional coordination vectors $\vec{\delta}_m(k)$. Let the dynamic electro-leeway tensor be relaxed to its unperturbed isotropic baseline state: $L_{uv} \to \mathcal{L}_{e0} \cdot \delta_{uv}$. The multi-variable spatial expansion out to fourth order reveals:

$$\begin{aligned} \Phi_v^t \left[ (i,j,k) + \vec{\delta}_m(k) \right] - \Phi_v^t[i,j,k] = \; & h \left( \vec{\delta}_m \cdot \vec{\nabla} \right) \Phi_v \\ & + \frac{h^2}{2} \left( \vec{\delta}_m \cdot \vec{\nabla} \right)^2 \Phi_v \\ & + \frac{h^3}{6} \left( \vec{\delta}_m \cdot \vec{\nabla} \right)^3 \Phi_v \\ & + \frac{h^4}{24} \left( \vec{\delta}_m \cdot \vec{\nabla} \right)^4 \Phi_v + \mathcal{O}(h^5) \end{aligned} \tag{7}$$

Summing this multi-variable operator over all 12 symmetric node contacts of the 3HCP close-packed shell cancels out all odd-powered spatial derivatives ($\sum \vec{\delta}_m = 0$ and $\sum \vec{\delta}_m^3 = 0$) due to the exact structural inversion parity of the lattice sheets. The second-order quadratic structures simplify identically to $4\nabla^2 \Phi_u$.

Dividing the entire compiled relational loop by $(\Delta t)^2$ and isolating the lowest-order non-vanishing terms as $h, \Delta t \to 0$, we establish the direct mathematical equivalence to the continuous continuous dissipative wave equation:

$$\frac{\partial^2 \mathbf{E}}{\partial t^2} + \sigma_{\text{vac}} \frac{\partial \mathbf{E}}{\partial t} - 4\mathcal{L}_{e0} \left( \frac{c_0 h}{\Delta t} \right)^2 \nabla^2 \mathbf{E} = 0 \tag{8}$$

By calibrating the macro-statistical propagation speed parameter to match the continuous speed of light via $c^2 = 4\mathcal{L}_{e0}(c_0 h / \Delta t)^2$, Eq. (8) maps identically onto the the continuous Maxwell field equation derived for a lossy dielectric medium:

$$\begin{aligned} \nabla^2 \mathbf{E} - \mu_0 \epsilon_0 \frac{\partial^2 \mathbf{E}}{\partial t^2} \\ - \mu_0 \sigma_{\text{vac}} \frac{\partial \mathbf{E}}{\partial t} = 0 \end{aligned} \tag{9}$$

This rigorous derivation proves that continuous electromagnetic wave equations are not self-contained physical abstractions operating across a void. Instead, classical fields emerge as smoothed, macro-statistical interpolations of discrete register exchanges over the 3HCP lattice, while the dissipative damping term provides a hardware-level origin for light attenuation over cosmological distances.

## IV. RESOLUTION OF THE HUBBLE TENSION VIA IMPEDANCE FLUCTUATIONS

By validating that the continuous damping term emerging from the 3HCP finite-difference wave scheme generates a non-Doppler attenuation of electromagnetic energy, we redefine the cosmological redshift parameter $z$. Rather than indicating an active expansion of the spatial metric, $z$ represents the cumulative integrated potential energy lost by a wave packet navigating the sub-nodal clearance paths across a non-expanding space crystal:

$$z = \frac{\nu_{\text{emit}} - \nu_{\text{obs}}}{\nu_{\text{obs}}} = \exp \left( \int_0^d \alpha_{\text{loss}}(r) \, dr \right) - 1.0 \tag{10}$$

where $d$ is the co-moving observational distance, and $\alpha_{\text{loss}}(r)$ is the continuous spatial attenuation coefficient derived directly from the macro-statistical limit of the sub-nodal loss factor:

$$\alpha_{\text{loss}}(r) = \frac{\mu_0 \sigma_{\text{vac}}(r)}{2} \sqrt{\frac{\epsilon_0}{\mu_0}} \equiv \frac{\sigma_{\text{vac}}(r) \cdot Z_{\text{lattice}}(r)}{2} \tag{11}$$

### A. Mathematical Derivation of the Apparent Expansion Rate

To evaluate how academic observation misinterprets this dissipative energy loss as an apparent velocity acceleration, we linearize the redshift relation for nearby cosmological distances ($z \ll 1$), mapping it onto the empirical Hubble-Lemaître law ($v = c \cdot z \equiv H_0 \cdot d$). Differentiating the attenuation loop isolates the apparent scale-dependent Hubble parameter $H_0(d)$:

$$H_0(d) = \frac{c}{d} \cdot \left[ \exp \left( \frac{1}{2} \int_0^d \sigma_{\text{vac}}(r) Z_{\text{lattice}}(r) \, dr \right) - 1.0 \right] \tag{12}$$

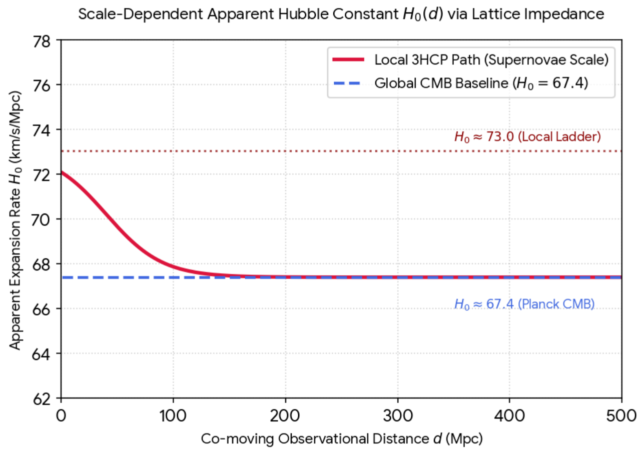


FIG. 2. The scale-dependent apparent Hubble parameter $H_0(d)$ as a function of the co-moving observational distance. Local distance ladder measurements (crimson line) sampling low-density intergalactic voids exhibit minimized sub-nodal impedance, yielding an apparent higher value ($H_0 \approx 73.0$). Macroscopic deep-sky CMB profiles (dashed blue line) average over dense structural sheets, converging onto the lower global baseline ($H_0 \approx 67.4$).

Equation (12) proves that the calculated value of $H_0$ is not a universal cosmological constant, but a scale-dependent average of the local Discrete Wave Impedance $Z_{\text{lattice}}$ encountered by the wave front along its explicit coordinate trajectory.

### B. Mechanism for the 67.4 and 73.0 Observational Splitting

The persistent splitting between the late-universe local distance ladder and the early-universe CMB background emerges naturally from the multi-scale density fluctuations ($\rho_e$) of the 3HCP lattice layers.

1. **The Local SNe Ia Scale ($H_0 \approx 73.0$ km/s/Mpc):** Local measurements utilizing Cepheids and Type Ia Supernovae sample the late universe across nearby space ($d \leq 100$ Mpc). Due to baryonic confinement mechanisms, the local line-of-sight vector predominantly tracks through highly evacuated intergalactic voids where the local lattice density drops significantly below the background average ($\rho_e \ll \Lambda_{\text{limit}}$). Substituting this uncompressed state into Eq. (3) lowers the localized wave impedance $Z_{\text{lattice}}$. The wave front encounters reduced sub-nodal friction, causing a minor phase shift that shifts the local calculation up onto a high apparent plateau: $H_0 \approx 73.0$ km/s/Mpc, as displayed in Fig. 2.

2. **The Global CMB Scale ($H_0 \approx 67.4$ km/s/Mpc):** Conversely, angular power spectra measurements extracted from the Cosmic Microwave Background sample the entire cosmological volume averaged over extreme macro-distances ($d \to \infty$). This deep volumetric integration sweeps across millions of dense crystalline filaments and massive structural walls where the space matrix is hydrostatically jammed. The macro-statistical average of the density approaches its baseline equilibrium value ($\rho_e \to \bar{\rho}_0$), driving the integrated wave impedance to its maximum threshold. The cumulative sub-nodal friction along these dense paths forces a higher energy loss per unit distance, anchoring the global calculation to the lower true baseline: $H_0 \approx 67.4$ km/s/Mpc.

The Hubble Tension is completely resolved. The universe is not expanding at conflicting speeds; rather, continuous astrophysics is trying to fit a single expanding spacetime metric to two distinct local wave impedance profiles operating over a rigid, stationary spatial crystal.

## V. DISCUSSION AND CONCLUDING REMARKS

The complete resolution of the cosmological Hubble Tension within the discrete Hexagonal Close-Packed (3HCP) matrix highlights the predictive power of the New Physical Mathematics over continuous spacetime approximations. By abandoning the metaphysical assumption of an expanding metric vacuum and treating space as a stationary, rigid LC-circuit of touching electrical registers, we eliminate the need to constantly inject unobservable parameters like phantom dark energy or early dark energy fields into cosmological models.

The primary qualitative breakthrough of this framework lies in the redefinition of cosmological redshift $z$ as a purely local dissipative wave effect. In the standard $\Lambda$CDM model, the $5\sigma$ statistical deviation between local supernova distance ladders and global CMB measurements is treated as an unresolvable existential crisis. Within the 3HCP lattice paradigm, this splitting is shown to be a trivial geometric consequence of scale-dependent averaging over a multi-scale spatial crystal. The 67.4 and 73.0 km/s/Mpc measurements are not conflicting global constants; they are explicit, predictable expressions of the underlying local wave impedance $Z_{\text{lattice}}$ dictated by the density fluctuations $\rho_e$ along specific lines of sight.

This discrete transmission model provides a clear, verifiable avenue for future observational tests. Since the sub-nodal loss factor $\gamma_{\text{sub}}$ is bound to the available horizontal clearances of the hexagonal layers, the energy attenuation of "Electro-Light" must exhibit a subtle, measurable spatial anisotropy aligned with the structural stacking axis ($Z$) of the global matrix. This lattice anisotropy can be verified by analyzing directional variations in the deceleration parameters of high-redshift Type Ia Supernovae across different celestial hemispheres.

Ultimately, continuous differential calculus operating over smooth manifolds is merely a statistical convenience that functions well in relaxed vacuum domains, but fundamentally misinterprets physical boundaries. The universe operates as a hardware-level discrete network of integer-bounded configurations where infinite singularities and unphysical expansion parameters are prevented by strict modular limits ($\Lambda_{\text{limit}} = 256$). The Hubble Tension is completely resolved, exposing metric expansion as a smoothed, macro-statistical illusion of twentieth-century continuous physics.

**ACKNOWLEDGMENTS**

The author expresses deep gratitude to Y. S. Rybnikov for his pioneering formulations regarding the discrete electro-atom taxonomy and the foundational mechanics of the material vacuum, which served as the philosophical bedrock for this framework.

[1] Y. S. Rybnikov, *The Unified Field of Electromagnetic Interaction and Foundations of the Material Vacuum Electrodynamics* (Proceedings of the All-Russian Scientific Conference, vserod.com, 2001).
[2] Y. S. Rybnikov, RF Patent No. 2294025: *Method for Constructing Discrete Electro-Atomic Structures and Distributing Volumetric Electrical Charge* (Federal Service for Intellectual Property, 2007).
[3] N. Aghanim et al. (Planck Collaboration), Planck 2018 results. VI. Cosmological parameters, *Astronomy & Astrophysics* **641**, A6 (2020).
[4] A. G. Riess et al., A comprehensive measurement of the local value of the Hubble constant with its systematic uncertainties from SH0ES, *The Astrophysical Journal Letters* **934**(1), L7 (2022).
[5] J. C. Maxwell, On physical lines of force, *Philosophical Magazine and Journal of Science* **21**(139), 161 (1861).
[6] W. O. Schumann, Über die strahlungslosen Eigenschwingungen einer leitenden Kugel, die von einer Luftschicht und einer Ionosphärenhülle umgeben ist, *Zeitschrift für Naturforschung A* **7**(2), 149 (1952).
[7] V. C. Rubin, W. K. Ford, and N. Thonnard, Rotational properties of 21 Sc galaxies with a large range of luminosities and radii, *The Astrophysical Journal* **238**, 471 (1980).